Review

Kenji Uchino*

Piezoelectric Actuator Renaissance

Abstract: "Politico-engineering" in the twenty-first century is generating "Piezoelectric Actuator Renaissance" in the area of sustainability and crisis technologies in particular. This paper reviews the recent advances in materials, designing concepts, and new applications of piezoelectric actuators and describes the future perspectives of this area.

Keywords: piezoelectric actuator, politico-engineering, efficiency, sustainability technology, energy harvesting, multi-functional

***Corresponding author: Kenji Uchino,** Department of Electrical Engineering, The Penn State University, University Park, PA, USA; ONR Global-Asia, Office of Naval Research (ONR), Roppongi, Minato-Ku, Tokyo 106-0032, Japan, E-mail: KenjiUchino@psu.edu, kenji.uchino.civ@mail.mil

Introduction

Actuator applications of piezoelectrics started in late 1970s, and enormous investment was installed on practical developments during 1980s, aiming at consumer applications such as precision positioners with high strain materials, multilayer device designing and mass-fabrication processes for portable electronic devices, ultrasonic motors for micro-robotics, and smart structures. After the slump due to the worldwide economic recession in 1990s, we are now facing a sort of "Renaissance" of piezoelectric actuators, according to the social environmental changes. The twenty-first century faces to a "sustainable society". Global regulations are strongly called on ecological and human health care issues, and the government-initiated technology (i.e. "politico-engineering") has become essential (Uchino 2012). Because of significantly high energy efficiency of piezoelectrics in comparison with other actuators such as chemical engines and electromagnetic components, piezoelectric actuators have been re-focused most recently in the sustainable society (i.e. Renaissance in piezoelectric actuators). This paper reviews the recent advances in materials, designing concepts, and new applications of piezoelectric actuators/transducers and describes the future perspectives of this area.

Historical background

Piezoelectricity was discovered by Jacque and Pierre Curie in 1880 in a quartz single crystal. Though the shipwreck of "Titanic" in 1912 motivated the application of piezoelectrics to sonar transducers to survey the undersea, we needed to wait for the real investment until World War I (1914–1918). Paul Langevin developed underwater transducers (so-called "Langevin Transducers") by sandwiching tiny quartz single crystals with metal plates in order to survey the German U-Boats (submarines). Another epoch-making discovery in piezoelectrics is a new ceramic, barium titanate, during World War II (WWII; 1939–1945). $BaTiO_3$ (BT) was firstly developed for creating high-capacitance materials for compact radar system applications, based on "Tita-Con" (then famous TiO_2-based condenser) independently by researchers in the US, Japan, and Russia (Wainer and Salomon 1946; Ogawa 1947; Vul 1946). The discovery of piezoelectricity on BT after electric-poling treatment by R. P. Gray facilitated wide application of piezoceramics after WWII (Jaffe, Cook, and Jaffe 1971). Lead zirconate titanate (PZT) with a monomorphic crystal structure (i.e. perovskite) was systematically studied (Sawaguchi 1953), and the piezoelectric performance was improved significantly in comparison with BT. The PZT has still been the most dominant piezoelectric materials in these 50 years.

After WWII, the country power (GDP) changed with year for Japan, USA (20 years ahead), and China (30 years behind) in a typical S-shape growth curve, as visualized in Figure 1. Let us review the product planning strategy taken historically by the Japanese industries. In 1960s, the four-Chinese-character slogan was "重厚長大 (*heavier thicker longer and larger*)"; that is, manufacturing heavier ships, thicker steel plates, constructing longer buildings, and larger power plants (dams) were the key strategies for recovering from the ruins of WWII (i.e. Domestic

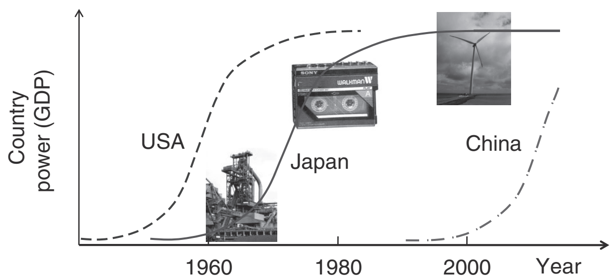

Figure 1 Country power (GDP) change with year for Japan, USA (20 years ahead), and China (30 years behind) visualized by typical S-shape growth curves (Uchino 2012)

Politics). Refer to the initial rise of the growth curve in Figure 1. Though Japanese people became wealthy, subsidiary effects started to surface: i.e. "industrial pollution". Steel industries produced air pollution which causes "asthma" even for small kids. Traffic congestion generated severe acoustic noise even in suburban areas. One of the most advanced industries, nuclear power plants, leaked hazardous radio-active wastes multiple times. The "melt-down" accident of Three-Mile-Island, Pennsylvania happened in 1979.

A completely opposite slogan started in the 1980s; that is, "軽薄短小 (*lighter thinner shorter and smaller*)". Printers and cameras became lighter in weight, thinner computers and TVs (flat panel) gained popularity, printing time and information transfer period became shorter, and air-conditioners and tape recorders (e.g. "Walk-man" by SONY) were smaller. Though the serious industrial pollution diminished gradually during this period in proportion to the country power (high GDP per person), different subsidiary effects started: (1) "greenhouse effect" and "global warming" due to CO_2 gas generated by over-produced automobiles, (2) energy crisis due to over-consumption of energy and lack of fossil energy sources (oil), in addition to the political mismanagement, and (3) population growth due to advanced medical technologies. Longer life time is welcomed by individuals (now the average age for Japanese female is approaching to 86, male, 81 already; the world-eldest). However, overpopulation of humans will create an imbalance against other animals/natures, and senior population, in particular, causes societal and economic problems (pension, health insurance, work force, etc.).

When the twenty-first century began, as a consequent result, environmental degradation, resource depletion, and food famine have become major problems. Global regulations (i.e. *global regime*) are strongly called, and the government-initiated technology, that is, politico-engineering has become further important again in order to overcome the regulations. On the other hand, "multinational terrorist attacks" have risen after the "Cold War" ending. The author proposed a new four-Chinese-character keyword for the era of politico-engineering, "協守減維 (cooperation protection reduction and continuation)" (Uchino 2012). Global coordination and international cooperation in standardization of internet systems and computer cables became essential to accelerate the mutual communication. The Kyoto Protocol in December 1997 is an international agreement linked to the United Nations Framework Convention on Climate Change for reducing greenhouse gas emission (http://unfccc.int/kyoto_protocol/items/2830.php). Protection of the territory and environment from the enemy or natural disaster and from infectious disease spread is mandatory. Reduction of toxic materials, such as lead, heavy metals, and dioxin, and of the use of resources and energy consumption is also the key, and the society continuation, i.e. status quo or sustainable society, is important to promote.

Advanced research trends

I will discuss five key trends in this paper for providing the future perspectives of research trends: "performance to reliability", "hard to soft", "macro to nano", "homo to hetero", and "single to multi-functional".

Performance to reliability

Lead-free piezoelectrics

In 2006, European Community started RoHS (Restrictions on the use of certain Hazardous Substances), which explicitly limits the usage of lead (Pb) in electronic equipments. Pb-free piezoceramics have started to be developed after 1999, which are classified basically into three groups: (Bi, Na)TiO_3 (BNT), (Na, K)NbO_3 (NKN), and tungsten bronze (TB), most of which are revival materials after 1970s.

The share of the patents for bismuth compounds (bismuth layered type and BNT type) exceeds 61%. This is because bismuth compounds are easily fabricated in comparison with other compounds. Honda Electronics, Japan developed Langevin transducers with the BNT-based ceramics for ultrasonic cleaner applications (Tou et al. 2009). Their composition $0.82(Bi_{1/2}Na_{1/2})TiO_3–0.15BT–0.03(Bi_{1/2}Na_{1/2})(Mn_{1/3}Nb_{2/3})O_3$ exhibits $d_{33} = 110 \times 10^{-12}$ C/N, which is only 1/3 of that of a hard PZT, but the electromechanical coupling factor $k_t = 0.41$ is larger because of much smaller permittivity ($\varepsilon = 500$) than that of the PZT. Furthermore, the maximum vibration velocity of a rectangular plate (k_{31} mode) is close to 1 m/s (rms value), which is higher than that of hard PZTs.

NKN systems exhibit the highest performance among the present Pb-free materials, because of the morphotropic phase boundary usage. Figure 2 shows the current best data reported by Toyota Central Research Lab, where strain curves for oriented and unoriented (K,Na,Li) (Nb, Ta,Sb)O_3 ceramics are shown (Saito 1996). Note that the maximum strain reaches up to $1{,}500 \times 10^{-6}$, which is equivalent to the PZT strain. Drawbacks include their sintering difficulty and the necessity of the sophisticated preparation technique (topochemical method for preparing flaky raw powder).

TB types are another alternative choice for resonance applications, because of their high Curie temperature and low loss. Taking into account general consumer attitude on disposability of portable equipment, Taiyo Yuden, Japan developed micro-ultrasonic motors using non-Pb multilayer piezo-actuators (Doshida 2009). Their composition is based on TB ($(Sr,Ca)_2NaNb_5O_{15}$) without heavy metal. The basic piezoelectric parameters in TB ($d_{33} = 55$–80 pC/N, $T_C = 300°C$) are not very attractive. However, once the *c*-axis oriented ceramics are prepared, the d_{33} is dramatically enhanced up to 240 pC/N. Further, since the Young's modulus $Y_{33}^E = 140$ GPa is more than twice of that of PZT, the higher generative stress is expected, which is suitable to ultrasonic motor applications. Taiyo Yuden developed a sophisticated preparation technology for oriented ceramics with a multilayer configuration: that is, preparation under strong magnetic field, much simpler than the flaky powder preparation.

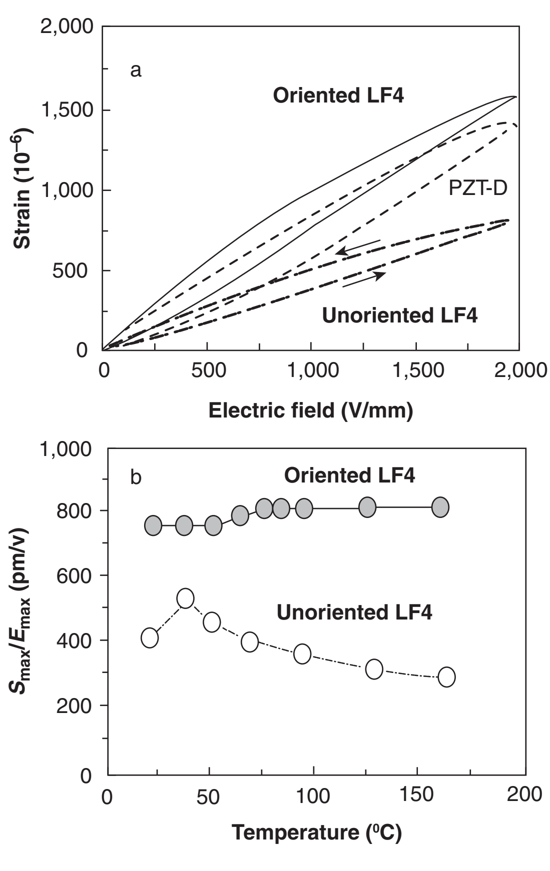

Figure 2 Strain curves for oriented and unoriented (K,Na,Li) (Nb,Ta, Sb)O_3 ceramics (Saito 1996)

Bio-degradable polymer

The above Pb-free materials are non-toxic and disposable. Murata Manufacturing Co. is further seeking biodegradable devices with L-type poly-lactic acid (PLLA). PLLA is made of vegetable corn based composition (www.murata.co.jp/corporate/ad/article/metamorphosis16/Application_note/). Because it exhibits pure piezoelectric without pyroelectric effect, the stress sensitivity is sufficient for leaf-grip remote controllers, which do not need a very long life time.

Low-loss piezoelectrics

High-power piezoelectrics with low loss have become a central research topic from the energy-efficiency improvement viewpoint; that is to say, "real (strain magnitude) to imaginary performance (heat generation reduction)". Reducing hysteresis and increasing the mechanical quality factor to amplify the resonance displacement is the primary target from the transducer application viewpoint. We proposed a universal loss characterization methodology in smart materials, piezoelectrics, and magnetostrictors; namely, by measuring accurately the mechanical quality factors Q_A for the resonance and Q_B for the antiresonance in the admittance/impedance curve, we can derive physical losses (Zhuang et al. 2010; Uchino, Zhuang, and Ural 2011).

There are three losses in piezoelectrics: dielectric tan δ, elastic tan φ, and piezoelectric tan θ, each of which is further categorized intensive (observable) and extensive (material parameter) losses as defined by:

$$\varepsilon^{X^*} = \varepsilon^X(1 - j\tan\delta'), s^{E^*} = s^E(1 - j\tan\phi'),$$
$$d^* = d(1 - j\tan\theta'), K^{X^*} = K^x(1 + j\tan\delta)$$
$$C^{D^*} = C^D(1 + j\tan\phi), h^* = h(1 + j\tan\theta).$$

Though the previous researchers neglected the piezoelectric loss (tan θ), we pointed out that piezoelectric loss has almost a comparable magnitude with the dielectric and elastic losses and is essential to explain the admittance/impedance spectrum.

A universal method for determining the piezoelectric loss is summarized for a piezoelectric sample here (e.g. k_{31} mode):

(1) Obtain tan δ' from an impedance analyzer or a capacitance meter at a frequency away from the resonance or antiresonance range;
(2) Obtain the following parameters experimentally from an admittance/impedance spectrum around the resonance (A-type) and antiresonance (B-type) range: ω_a, ω_b, Q_A, Q_B (from the 3-dB bandwidth method), and the normalized frequency $\Omega_b = \omega_b l/2v$;
(3) Obtain tan φ' from the inverse value of Q_A (quality factor at the resonance) in the k_{31} mode;
(4) Calculate electromechanical coupling factor k from the ω_a and ω_b with the IEEE Standard equation in the k_{31} mode:

$$\frac{k_{31}^2}{1-k_{31}^2} = \frac{\Pi}{2}\frac{\omega_b}{\omega_a}\tan\left[\frac{\Pi(\omega_b-\omega_a)}{2\omega_a}\right]; \qquad [1]$$

(5) Finally obtain tan θ' by the following equation in the k_{31} mode:

$$\tan\theta' = \frac{\dfrac{\tan\delta' + \tan\phi'}{2} + \dfrac{1}{4}\left(\dfrac{1}{Q_A} - \dfrac{1}{Q_B}\right)}{\left[1 + \left(\dfrac{1}{k_{31}} - k_{31}\right)^2 \Omega_b^2\right]} \qquad [2]$$

High-power characterization of Pb-free piezoelectric and PZT disk samples is shown in Figure 3, where the resonance Q_A and antiresonance Q_B are plotted as a function of vibration velocity. Compared with the maximum vibration velocity (defined by the velocity which generates 20°C temperature rise on the sample) of 0.3 m/s (rms) in hard PZT, Pb-free piezoelectrics can exhibit the maximum vibration velocity higher than 0.5 m/s, triple higher energy density as a transducer.

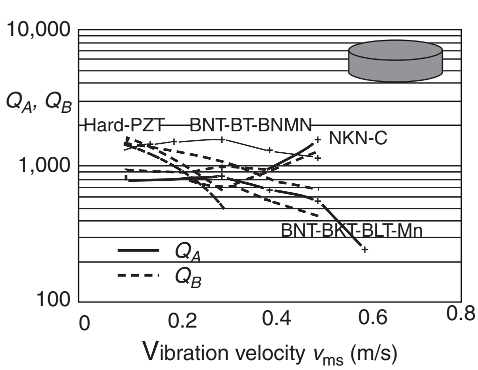

Figure 3 High-power characterization of Pb-free piezoelectrics and PZT. Maximum vibration velocity is larger for Pb-free materials

Hard to soft

We are facing the revival polymer era after 1980s because of their elastically soft superiority. Larger, thinner, lighter, and mechanically flexible human interfaces are the current necessity in the portable electronic devices, leading to the development in elastically soft displays, electronic circuits, and speakers/microphones.

(i) Elastomer actuators: Dielectric elastomer actuators (non-piezoelectric and non-ferroelectric) are based on the deformation of a soft polymer which acts as a dielectric between highly compliant electrodes. This effect is dominated by the Maxwell's stresses imposed by the compliant electrodes. Extremely high strains at low frequencies have been reported by Pelrine et al. (2000). In-plane strains of more than 100% and 200% were observed in silicone and acrylic elastomers, respectively.
(ii) Electrostrictive polymers: Polyvinylidene difluoride-trifluoroethylene (PVDF-TrFE) copolymer is a well-known piezoelectric, which has been popularly used in sensor applications such as keyboards. Zhang et al. reported that the field induced strain level can be significantly enhanced up to 5% using a high-energy electron irradiation onto the PVDF films, leading to an electrostrictive performance (Bharti et al. 2000).
(iii) 1:3 PZT composites: Fuji Film news released their new bendable and foldable speakers with a 1:3 composite (PZT fine powder was mixed in a polymer film) (http://techon.nikkeibp.co.jp/english/NEWS_EN/20130201/263651/). Superior acoustic performance seems to be promising for flat-speaker applications.
(iv) Large strain ceramics: $Pb(Zn_{1/3}Nb_{2/3})O_3$–$PbTiO_3$ (PZN–PT) or $Pb(Mg_{1/3}Nb_{2/3})O_3$–$PbTiO_3$ (PMN–PT) single crystals became focused due to the rubber-like-soft piezoceramic strain after 25 years of the discovery. Since the enhancement of the induced strain level is a primary target, single crystals with a better capability for generating larger strains are being used in these days. In 1981, Kuwata et al. firstly reported an enormously large electromechanical coupling factor k_{33} = 92–95% and piezoelectric constant d_{33} = 1,500 pC/N in solid solution

single crystals between relaxor and normal ferroelectrics, PZN–PT (Kuwata, Uchino, and Nomura 1981; Kuwata, Uchino, and Nomura 1982). This discovery has been marked practically after more than 15 years when high k materials have been paid attention in medical acoustics. These data have been reconfirmed, and improved data were obtained recently, aiming at medical acoustic applications (Yanagiwawa, Kanai, and Yamashita 1995; Park and Shrout 1997). The strains as large as 1.7% can be induced practically for the PZN–PT solid solution single crystals (Figure 4). It is notable that the highest values are observed for a rhombohedral composition only when the single crystal is poled along the perovskite [0 0 1] axis, not along the [1 1 1] spontaneous polarization axis.

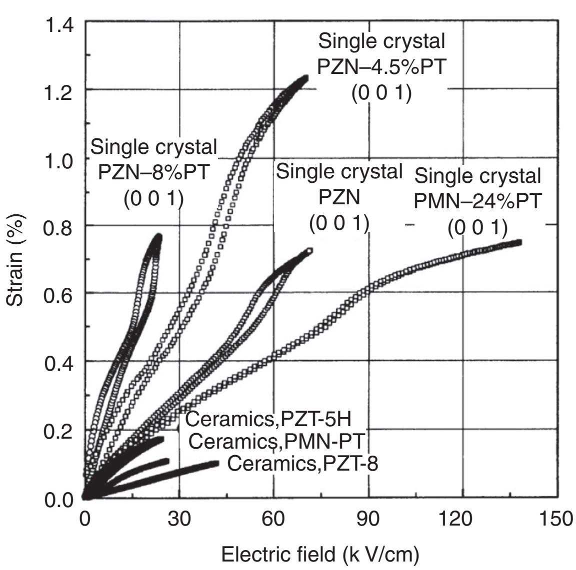

Figure 4 Field induced strains in single crystals $Pb(Zn_{1/3}Nb_{2/3})O_3$–$PbTiO_3$ in comparison with PZT ceramics (Park and Shrout 1997)

Macro to nano

In the micro(nano)-electro-mechanical system (MEMS/NEMS) area, *piezoelectric-MEMS* is one of the miniaturization targets for integrating the piezo-actuators in a micro-scale device, aiming at bio/medical applications for maintaining the human health.

PZT thin films are deposited on a silicon wafer, which is then micro-machined to leave a membrane for fabricating micro-actuators and -sensors, i.e. micro-electromechanical systems. Figure 5 illustrates a blood tester developed by The Penn State in collaboration with OMRON Corporation, Japan (Kalpat 2001). Applying voltage to two surface interdigital electrodes, the surface PZT film generates surface membrane waves, which soak up blood and the test chemical from the two inlets, then mix them in the center part, and send the mixture to the monitor part through the outlet. Finite Element Analysis (FEA) calculation was conducted to evaluate the flow rate of the liquid by changing the thickness of the PZT or the Si membrane, inlet and outlet nozzle size, and cavity thickness. Refer to (Tadigadapa and Mateti 2009) for the up-dated piezoelectric-MEMS studies.

Homo to hetero

Homo to hetero structure change is also a recent research trend: stress-gradient in terms of space in a dielectric material exhibits piezoelectric-equivalent sensing capability (i.e. “flexoelectricity”), while electric-field gradient in terms of space in a semiconductive piezoelectric can exhibit bimorph-equivalent flextensional deformation (monomorph).

Space gradient of stress or electric field generates direct or converse flexoelectric effect expressed, respectively, by

$$\boldsymbol{P}_{\mathrm{l}} = \mu_{ijkl}(\partial \boldsymbol{x}_{\mathrm{ij}}/\partial x_k), \quad [3]$$

$$\boldsymbol{X}_{\mathrm{ij}} = \mu_{ijkl}(\partial \boldsymbol{E}_{\mathrm{l}}/\partial x_k), \quad [4]$$

where $\boldsymbol{P}_{\mathrm{l}}$ and $\boldsymbol{E}_{\mathrm{l}}$ are electric polarization and electric field, respectively; $\boldsymbol{X}_{ij}$ and $\boldsymbol{x}_{ij}$ are elastic stress and strain, respectively; x_k is coordination in $\boldsymbol{x}_{ij}$ or $\boldsymbol{E}_{\mathrm{l}}$; μ_{ijkl} is denoted as a flexoelectric coefficient, which has a fourth rank polar tensor symmetry, similar to the electrostrictive tensor (Tagantsev 1986). This means that even a paraelectric material can generate charge under stress when the strain gradient is generated artificially in the material. Cross et al. demonstrated this “piezoelectric”-equivalent effect in various artificial designs as shown in Figure 6. $Ba_{0.67}Sr_{0.33}TiO_3$ (BST) paraelectric composition sample with a trapezoid shape exhibited 10^{-7} C/m^2 of polarization under a strain gradient of 10^{-3}/m.

Conventional bimorph bending actuators are composed of two piezoelectric plates, or two piezoelectrics and an elastic shim, bonded together. The bonding layer in the latter, however, causes both an increase in hysteresis and a degradation of the displacement characteristics, as well as delamination problems. Furthermore, the fabrication process for such devices, which involves cutting, polishing, electroding, and bonding steps, is rather laborious and costly. Thus, a monolithic bending actuator (monomorph) that requires no bonding is a very attractive alternative structure.

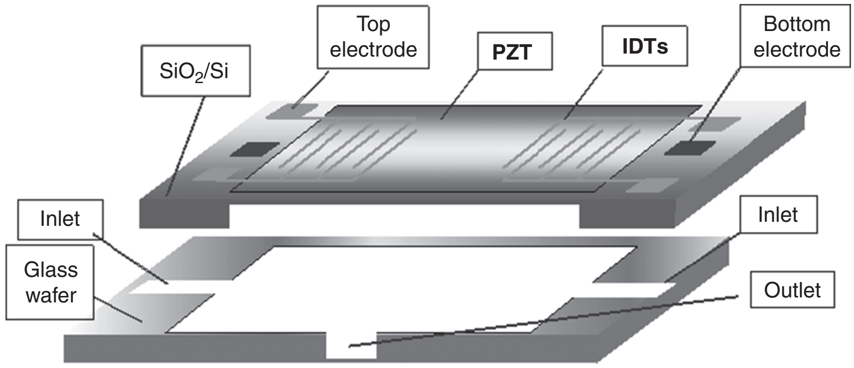

Figure 5 Structure of a PZT/silicon MEMS device, blood tester (Kalpat 2001)

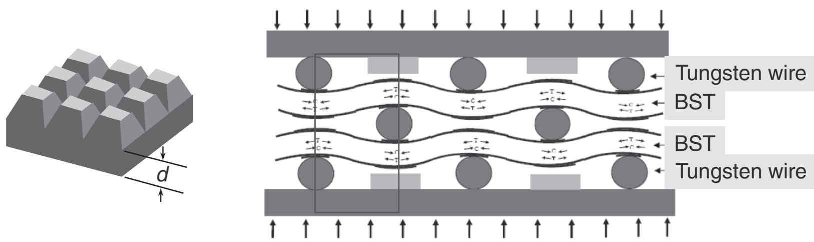

Figure 6 Space gradient of stress can be obtained in trapezoidal BST samples or wire-inserted BST laminates

Such a monomorph device can be produced from a single ceramic plate (Uchino et al. 1987). The operating principle is based on the combined action of a semiconductor contact phenomenon and the piezoelectric or electrostrictive effect. When metal electrodes are applied to both surfaces of a semiconductor plate and a voltage is applied as shown in Figure 7, the electric field is concentrated on one side (i.e. "Schottky barrier"), thereby generating a non-uniform field within the plate. When the piezoelectric (or electrostrictor) is slightly semiconductive, contraction along the surface occurs through the piezoelectric effect only on the side where the electric field is concentrated. The non-uniform field distribution generated in the ceramic causes an overall bending of the entire plate. The energy diagram of a modified structure including a very thin insulative layer is represented in Figure 8(a) (Uchino, Yoshizaki, and Nagao 1987). The thin insulator layer increases the breakdown voltage. The *rainbow actuator* by Aura Ceramics is a modification of the basic semiconductive piezoelectric monomorph design, where half of the piezoelectric plate is reduced so as to make a thick semiconductive electrode which enhances the bending action (Aura Ceramics, Inc., USA, Catalogue "Rainbow"). The energy diagram for the "rainbow" device is shown in Figure 8(b) (Uchino, Yoshizaki, and Nagao 1987).

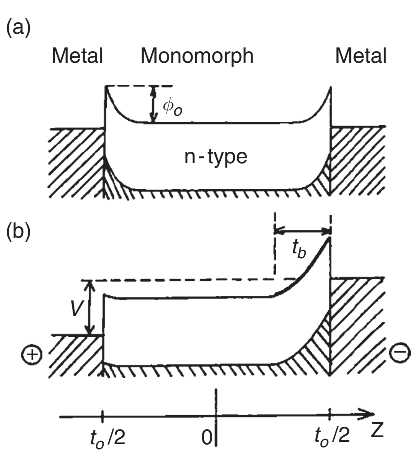

Figure 7 Schottky barrier generated at the interface between a semiconductive (n-type) piezoceramic and metal electrodes

Single to multi-functional

Some new functions can be realized by coupling two effects. We developed magnetoelectric devices (i.e. voltage is generated by applying magnetic field) by laminating magnetostrictive Terfenol-D and piezoelectric PZT materials and demonstrated photostriction by coupling photovoltaic and piezoelectric effects in Lanthunam-doped PZT (PLZT).

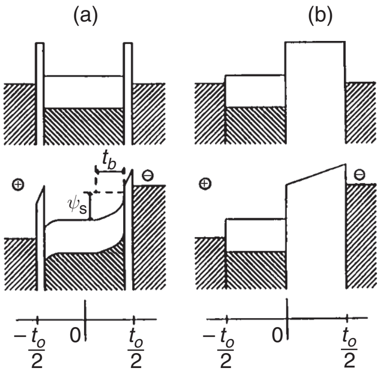

Figure 8 Energy diagrams for modified monomorph structures: (a) a device incorporating a very thin insulating layer and (b) the rainbow structure

Magnetoelectric effect

Similar to nuclear radiation, magnetic irradiation cannot be easily felt by human. We cannot even purchase a magnetic field detector for a low frequency (50 or 60 Hz). The Penn State, in collaboration with Seoul National University, developed a simple and handy magnetic noise sensor for these environmental monitoring purpose, e.g. below a high-voltage power transmission line. Figure 9 shows a schematic structure of this device, in which a PZT disk is sandwiched by two Terfenol-D (magnetostrictor) disks (Ryu et al. 2001). When a magnetic field is applied on this composite, Terfenol will expand, which is mechanically transferred to PZT, leading to an electric charge generation from PZT. By monitoring the voltage generated in the PZT, we can detect the magnetic field. The key of this device is highly effective for a low frequency such as 50 Hz (Ryu et al. 2001).

Photostriction

A photostrictive actuator is a fine example of an intelligent material, incorporating "illumination sensing" and self-production of "drive/control voltage" together with final "actuation". In certain ferroelectrics, a constant electromotive force is generated with exposure of light, and a photostrictive strain results from the coupling of this bulk photovoltaic effect with inverse piezoelectricity. A bimorph unit has been made from PLZT 3/52/48 ceramic doped with slight addition of tungsten (Uchino 1997). The remnant polarization of one PLZT layer is parallel to the plate and in the direction opposite to that of the other plate. When a violet light is irradiated to one side of the PLZT bimorph, a photovoltage of 1 kV/mm is generated, causing a bending motion. The tip displacement of a 20-mm bimorph with 0.4 mm in thickness was 150 µm, with a response time of 1 s.

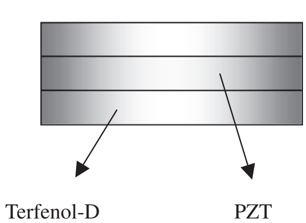

Figure 9 Magnetic noise sensor consisting of a laminated composite of a PZT and two Terfenol-D disks (Ryu et al. 2001)

A photo-driven micro-walking device, designed to begin moving by light illumination, has been developed (Uchino 1989). As shown in Figure 10, it is simple in structure, having neither lead wires nor electric circuitry, with two bimorph legs fixed to a plastic board. When the legs are irradiated alternately with light, the device moves like an inchworm with a speed of 100 µm/min. In pursuit of thick film type photostrictive actuators for space structure applications, in collaboration with Jet Propulsion Laboratory, The Penn State investigated the optimal range of sample thickness and surface roughness dependence of photostriction. Thirty-micrometer-thick PLZT films exhibit the maximum photovoltaic phenomenon (Poosanaas, Tonooka, and Uchino 2000).

New application developments

Normal technologies

One of the *normal technologies*, which are initiated politically, is the sustainability technology. The sustainability technologies include:

- Power and energy (lack of oil, nuclear power plant, and new energy harvesting)
- Rare material (rare-earth metal and lithium)
- Food (rice and corn – bio-fuel)
- Toxic material
  - Restriction (heavy metal, Pb, and dioxin)
  - Elimination/neutralization (mercury and asbestos)
  - Replacement material
- Environmental pollution
- Energy efficiency

In the application area, the global regime for "ecological sustainability" particularly accelerated new developments in ultrasonic disposal technology of hazardous materials, diesel injection valves for air pollution, and piezoelectric renewable energy harvesting systems.

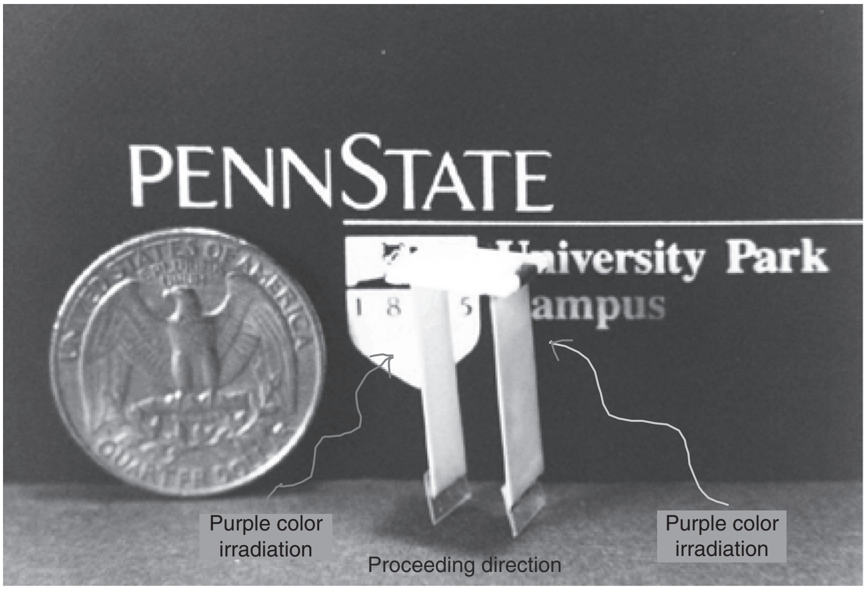

Figure 10 Photo-driven walking device with photostrictive PLZT bimorphs (Uchino 1989)

Ultrasonic disposal technology

Ultrasonic lens cleaner is commonly used in home. Industrial ultrasonic cleaners are widely utilized in the manufacturing lines of silicon wafers and liquid crystal glass substrates. Honda Electronics added another ultrasonic cleaner in conjunction with a washing machine produced by Sharp (Private Communication, Honda Electronics Company Brochure). Using an L–L coupler horn to generate water cavitation, their machine can remove dirt on a shirt collar. It is noteworthy that we can reduce the amount of detergent (one of the major causes of the river contamination) significantly by this technique.

With increasing the power level of water cavitation, we can make hazardous waste innocuous, because the cavitation (cyclic adiabatic compression) generates more than 3,000°C locally for a short period. Hazardous wastes in underground or sewer water include dioxin, trichloroethylene, PCB, and environmental hormone (Hua and Hoffmann 1997). As known well, dioxin becomes another toxic material when it is burned at a low temperature, while it becomes innocuous only when burned at a high enough temperature.

Reduction of contamination gas

Diesel engines are recommended rather than regular gasoline cars from the energy conservation and global warming viewpoint. When we consider the total energy of gasoline production, both well-to-tank and tank-to-wheel, the energy efficiency, measured by the total energy required to realize unit drive distance for a vehicle (MJ/km), is of course better for high octane gasoline than diesel oil. However, since the electric energy required for purification is significant, the gasoline is inferior to diesel (www.marklines.com/ja/amreport/rep094_200208.jsp).
As well known, the conventional diesel engine, however, generates toxic exhaust gases such as SO_x and NO_x. In order to solve this problem, new diesel injection valves were developed by Siemens, Bosch, and Toyota with piezoelectric multilayered actuators. Figure 11 shows such a common rail type diesel injection valve with a ML piezo-actuator which produces high pressure fuel

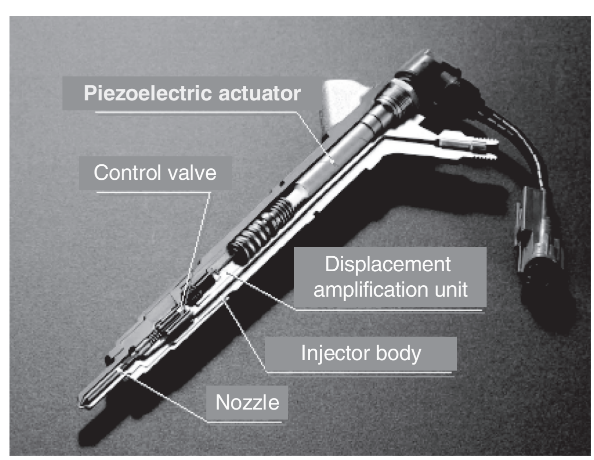

Figure 11 Common rail type diesel injection valve with a piezoelectric multilayer actuator [Courtesy by Denso Corporation]

and quick injection control. The highest reliability of these devices at an elevated temperature (150°C) for a long period (10 years) has been achieved (Fujii 2005). The piezoelectric actuator is namely the key to increase burning efficiency and minimize the toxic exhaust gases.

New energy harvesting systems

One of the most recent research interests is piezoelectric energy harvesting. Cyclic electric field excited in the piezoelectric plate by the environmental noise vibration is now accumulated into a rechargeable battery without consuming it as Joule heat. NEC-Tokin developed an LED traffic light array system driven by a piezoelectric windmill, which is operated by wind generated effectively by passing automobiles. Successful products (million sellers) in the commercial market include "Lightning Switch" (remote switch for room lights, with a unimorph piezoelectric component) by PulseSwitch Systems, VA (Uchino and Ishii 1988). In addition to the living convenience, Lightning Switch (Figure 12) can reduce the housing construction cost drastically, due to a significant reduction of the copper electric wire and the aligning labor.

The Penn State group developed energy harvesting piezoelectric devices based on a "cymbal" structure (29 mmϕ, 1- to 2-mm thick), which can generate electric energy up to 100 mW under an automobile engine vibration (Kim et al. 2005). By combining three cymbals in a rubber composite, a washer-like energy harvesting sheet was developed for a hybrid car application, aiming at 1-W power level constant accumulation to a fuel cell.

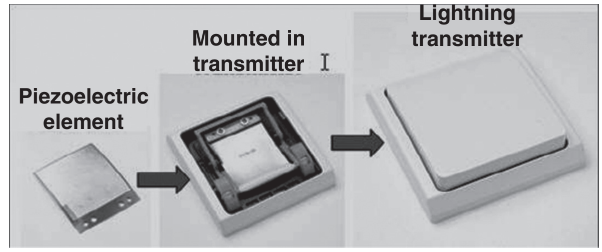

Figure 12 Lightning Switch with piezoelectric Thunder actuator. [Courtesy by Face Electronics]

These efforts have provided the initial research guidelines and have brought in light the problems and limitations of implementing the piezoelectric transducer. There are three major phases/steps associated with piezoelectric energy harvesting, as illustrated in Figure 13 (Uchino 2011): (i) mechanical–mechanical energy transfer, including mechanical stability of the piezoelectric transducer under large stresses, and mechanical impedance matching, (ii) mechanical–electrical energy transduction, relating with the electromechanical coupling factor in the composite transducer structure, and (iii) electrical–electrical energy transfer, including electrical impedance matching, such as a DC/DC converter to accumulate the energy into a rechargeable battery.

Let us discuss why the energy amount decreases with transmitting and transducing successively by numerical analyses, by referring to Table 1. The sample was a cymbal with 0.3-mm thick stainless steel endcaps, inserted below a 4 kg engine weight (40 N bias force). The electromagnetic shaker shook at 100 Hz for 8 s, and the

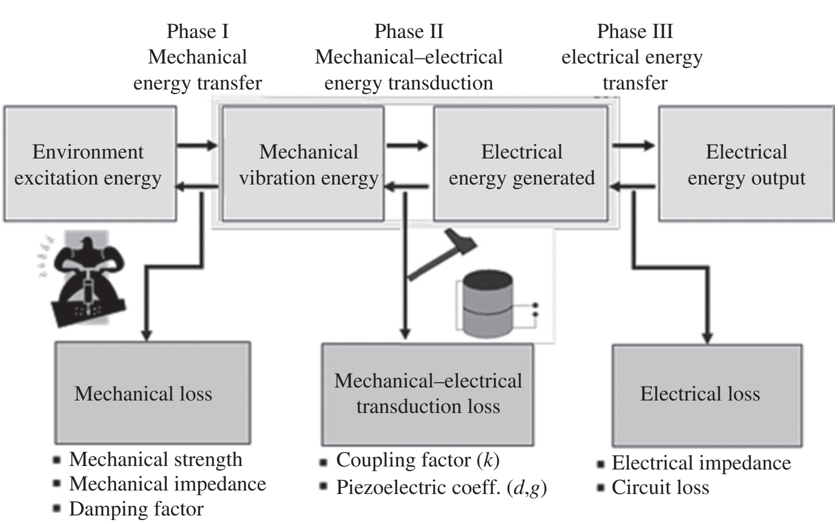

Figure 13 Three major phases associated with piezoelectric energy harvesting): (i) mechanical–mechanical energy transfer, (ii) mechanical–electrical energy transduction, and (iii) electrical–electrical energy transfer (Uchino 2011)

Table 1 Energy Flow/conversion analysis int the cymbal energy harvesting process (Uchino 2011)

Source Mechanical energy		Transducer Mechanical energy		Transducer Electrical energy		Circuit-in Electrical energy		Battery Electrical energy
9.48 J	⟶ ⟵	**8.22 J**	⟶ ⟵	**0.74 J**	⟶ ⟵	**0.42 J**	⟶ ⟵	**0.34 J**

accumulated energy during that time period was measured at each point.

Source to transducer: mechanical impedance mismatch

8.22 J/9.48 J = 87% of the mechanical energy is transmitted from the source to piezo-cymbal transducer. If the mechanical impedance is not seriously considered in the transducer (too mechanical-soft or -hard), the mechanical energy will not transfer efficiently, and large amount will be reflected at the contact/interface point.

Transduction in the transducer: electromechanical coupling

Transduction rate is evaluated by k^2. Since the $k_{eff} = 0.25$–0.30 in the cymbal, the energy conversion rate will be 9% maximum. The remaining portion will remain as the original mechanical vibration energy. 0.74 J/ 8.22 J = 9.0%. Since k_{eff} of the bimorph or unimorph is much smaller (10–15%), the energy conversion rate is smaller than 2%. Using modes with higher k values is highly recommended.

Transducer to harvesting circuit: electrical impedance matching

0.42 J/0.74 J = 57% is related with the electrical impedance mismatch between the cymbal output and the circuit input.

Harvesting circuit to rechargeable battery

0.34 J/0.42 J = 81%. This reduction is partially originated from the energy consumption in the circuit and partially originated from the electrical impedance mismatch between the circuit output (still around 5 kΩ) and the rechargeable battery impedance (around 10–20 Ω).

In summary, 0.34 J/9.48 J = 3.6% is the current energy harvesting rate from the vibration source to the storing battery. Losses in all the above phases should be taken into account, in order to increase the system efficiency.

Crisis technology

Politico-engineering covers (1) legally-regulated normal technologies such as sustainability, as discussed in the previous section and (2) crisis technologies which are further classified into five types of "crises" (Uchino 2012):

- Natural disasters (earthquakes, tsunamis, tornadoes, hurricanes, lightning, etc.),
- Epidemic/infectious diseases (smallpox, polio, measles, and HIV),
- Enormous accident (Three-Mile-Island core meltdown accident, BP oil spill etc.),
- Intentional accidents (acts of terrorism and criminal activity),
- Civil-war, war, territorial aggression.

As infectious or contagious disease involves some association with terrorist activities, those five are related to each other. In the United States, politicians were attacked with anthrax in 2001. In order to neutralize the biological attack, Pezeshk et al. at The Penn State University developed a portable hypochlorous acid disinfection device with a piezoelectric ultrasonic humidifier (Pezeshk, Gao, and Uchino 2004). Hypochlorous acid is a strong disinfectant with no side effect on humans and would be ideal for disinfecting office and hospital buildings against virus-caused diseases like SARS and anthrax. Coupled with the atomization of the acidic solution, much higher disinfection effects can be expected. This acid is not sold as a pure solution, since it naturally disintegrates after a few hours. We designed a corrosion-resistant electrolytic cell to produce hypochlorous acid from brine. An ultrasonic piezoelectric atomizer was utilized to generate micro-droplets of the diluted acid.

Regarding the natural disaster, the research themes of urgent need in the actuator/sensor area include: (1) prediction technologies such as for earthquakes and tornadoes, (2) accurate monitoring and surveillance techniques, (3) technologies for gathering and managing crisis information and informing the public in a way not to bring about panic reaction, and (4) rescue technologies (autonomous unmanned underwater, aerial, land vehicles, robots, etc.).

Until 1960s, the development of *weapons of mass destruction* was the primary focus, including nuclear bombs and chemical weapons. However, based on the global trend for "Jus in Bello (Justice in War)", *environment-friendly "green" weapons* became the main-stream in the twenty-first century; that is, minimal destructive weapons with a pin-point target such as laser guns and rail guns. In this direction, programmable air-burst munition was developed successfully from 2004. The 25-mm caliber "Programmable Ammunition" by ATK Integrated Weapon Systems, AZ and Micromechatronics, PA (http://www.atk.com/MediaCenter/mediacenter_ video gallery.asp) uses a multilayer piezo-actuator (instead of a battery) for generating electric energy under shot impact to activate the operational amplifiers which ignite the burst according to the command program.

Summary

We discussed five key trends in this paper for providing the future perspectives: performance to reliability (Pb-free piezoelectrics, bio-degradable piezo-polymer, and low-loss piezoelectric), hard to soft (foldable piezo-polymer film and PMN/PZN single crystals), "macro to nano" (piezo-MEMS), homo to hetero (flexoelectricity and monomorph), and single to multi-functional (magnetoelectrics and photostriction). In the application area, the global regime for ecological sustainability particularly accelerated new developments in ultrasonic disposal technology of hazardous materials, diesel injection valves for air pollution, and piezoelectric renewable energy harvesting systems. In crisis technology applications, piezoelectric energy harvesting is important also for pin-point target weapons.

Acknowledgments: The author would like to acknowledge the US Office of Naval Research for continuous research support to International Center for Actuators and Transducers at The Pennsylvania State University (N00014-99-1-0754, N00014-08-1-0912, and N00014-12-1-1044).

References

Bharti, V., H. S. Xu, G. Shanti, Q. M. Zhang, and K. Liang. 2000. "Polarization and structural properties of high-energy electron irradiated poly (vinylidene fluoride – trifluoro ethylene) copolymer films." *Journal of Applied Physics* 87:452.

Cross, L. E. 2006. "Flexoelectric effects: charge separation in insulating solids subjected to elastic strain gradients." *Journal of Materials Science* 41:53.

Doshida, Y. 2009. "Pb-Free piezoelectric actuators." Proceeding of the 81st Smart Actuators/Sensors Study Committee, Jttas, Tokyo, December 11.

Fujii, A. 2005. "Piezoelectric actuators for Diesel injection valve control." Proceedings of Jttas Meeting on December 2, Tokyo.

Hua, I., and M. R. Hoffmann. 1997. "Optimization of Ultrasonic Irradiation as an Advanced Oxidation Technology." *Environmental Science and Technology* 31(8):2237–43.

Jaffe, B., W. Cook, and H. Jaffe. 1971. *Piezoelectric Ceramics*. London: Academic Press.

Kalpat, S. 2001. Ph.D. thesis, "Sputtered Highly Oriented PZT Films for MEMS Devices." Penn State University, Fall.

Kim, H. W., S. Priya, K. Uchino, and R. E. Newnham. 2005. *Journal of Electroceramics* 15:27–34.

Kuwata, J., K. Uchino, and S. Nomura. 1981. "Phase Transitions on the $Pb(Zn_{1/3}nb_{2/3})O_3 – PbTiO_3$ System." *Ferroelectrics* 37:579–82.

Kuwata, J., K. Uchino, and S. Nomura. 1982. "Dielectric and Piezoelectric Properties of $0.91pb(Zn_{1/3}nb_{2/3})O_3–0.09PbTiO_3$ Single Crystals." *Japanese Journal of Applied Physics* 21:1298–302.

Ogawa, T. 1947. "On Barium Titanate Ceramics [in Japanese]." *Busseiron Kenkyu* 6:1–27.

Park, S. E., and T. R. Shrout. 1997. "Relaxor based ferroelectric single crystals for electro-mechanical actuators." *Material Research Innovations* 1:20.

Pelrine, R. E., R. D. Kornbluh, Q. Pei, and J. P. Joseph. 2000. "High-Speed Electrically Actuated Elastomers with Strain Greater Than 100%." *Science* 287:836.

Pezeshk, A., Y. Gao, and K. Uchino. 2004. "Ultrasonic Piezoelectric Hypochlorous Acid Humidifier for Disinfection Applications." *NSF EE REU Penn State Annual Research Journal* II. Isbn 0-913260-04-5.

Poosanaas, P., K. Tonooka, and K. Uchino. 2000. "Photostrictive Actuators." *Journal of Mechatronics* 10:467–87.

Ryu, J., A. Vazquez Carazo, K. Uchino, and H. E. Kim. 2001. "Magnetoelectric Properties in Piezoelectric and Magnetostrictive Laminate composites." *Japanese Journal of Applied Physics* 40:4948–51.

Saito, Y. 1996. "Measurement System for Electric Field – Induced Strain by Use of Displacement Magnification Technique." *Japanese Journal of Applied Physics* 35:5168–73.

Sawaguchi, E. 1953. "Ferroelectricity versus Anti-Ferroelectricity in the Solid Solutions of $PbZrO_3$ and $PbTiO_3$." *Journal of the Physical Society of Japan* 8:615–29.

Tadigadapa, S., and K. Mateti. 2009. “Piezoelectric Mems Sensors: State-of-the-Art and Perspectives.” *Measurement Science and Technology* 20:092001.
Tagantsev, A. K. 1986. “Piezoelectricity and Flexoelectricity in Crystalline Dielectrics.” *Physical Review B* 34:5883.
Tou, T., Y. Hamaguchi, Y. Maida, H. Yamamori, K. Takahashi, and Y. Terashima. 2009. “Properties of $(BiNa)TiO_3$–$BaTiO_3$–(BiNa) $(Mn_{1/3}Nb_{2/3})$ O_3 Pb-Free Piezoelectric Ceramics and its Application to Ultrasonic Cleaner.” *Japanese Journal of Applied Physics* 48:07GM03.
Uchino, K. 1989. “Micro Walking Machines Using Piezoelectric Devices.” *Journal of Robot Mechanics* 1(2):124–27.
Uchino, K. 1997. “New Applications of Photostrictive Ferroics.” *Materials Research Innovations* 1:163–68.
Uchino, K. 2011. “Energy Harvesting with Piezoelectric and Pyroelectric Materials.” In *Partial Charge Chapter 4 “Energy Flow Analysis in Piezoelectric Harvesting Systems*, edited by N. Muensit. Zuerich, Switzerland: Trans Tech Publications.
Uchino, K. 2012. “Politico-Engineering in Piezoelectric Devices.” Proceedings of the 13th Int’l Conference New Actuators, Bremen, Germany, June 18–20, A1.0.
Uchino, K., and T. Ishii. 1988. “Mechanical Damper Using Piezoelectric Ceramics.” *Journal of the Ceramic Society of Japan* 96(8):863–7.
Uchino, K., M. Yoshizaki, K. Kasai, H. Yamamura, N. Sakai, and H. Asakura. 1987. “‘Monomorph Actuators’ Using Semiconductive Ferroelectrics.” *Japanese Journal of Applied Physics* 26:1046–49.
Uchino, K., M. Yoshizaki, and A. Nagao. 1987. “Monomorph Characteristics of Semiconductive Piezoceramics.” *Japanese Journal of Applied Physics* 26(Suppl. 26–2):201–3.
Uchino, K., Y. Zhuang, and S. O. Ural. 2011. “Loss Determination Methodology for a Piezoelectric Ceramic: New Phenomenological Theory and Experimental Proposals.” *Journal of Advanced Dielectrics* 1(1):17–31.
Vul, B. M. 1946. “High and Ultrahigh Dielectric Constant Materials [in Russian].” *Electrichestvo* 3.
Wainer, E., and N. Salomon. 1946. “High Titania Dielectrics.” *Transactions of the Electrochemical Society* 89.
Yanagisawa, K., H. Kanai, and Y. Yamashita. 1995. “Hydrothermal crystal growth of Lanthanum – Modified Lead Zirconate Titanate.” *Japanese Journal of Applied Physics* 34:5946–48.
Zhuang, Y., S. O. Ural, S. Tuncdemir, A. Amin, and K. Uchino. 2010. “Analysis on Loss Anisotropy of Piezoelectrics with ∞Mm Crystal Symmetry.” *Japanese Journal of Applied Physics* 49:021503.